

## The Egion June 15, 1995 (6.2 $M_L$ ) Earthquake, Western Greece

G.-A. TSELENTIS,<sup>1</sup> N. S. MELIS,<sup>1</sup> E. SOKOS<sup>1</sup> and K. PAPATSIMPA<sup>1</sup>

*Abstract*—On June 15, 1995 at 00:15 GMT a devastating earthquake (6.2  $M_L$ ) occurred in the western end of the Gulf of Corinth. This was followed 15 min later by the largest aftershock (5.4  $M_L$ ). The main event was located by the University of Patras Seismological Network (PATNET) at the northern side of the Gulf of Corinth graben. The second event (5.4  $M_L$ ) was located also by PATNET near the city of Egion, on a fault parallel to the Eliki major fault that defines the south bound of the Gulf of Corinth graben. A seismogenic volume that spans the villages of Akrata (SE) and Rodini (NW) and extends to Eratini (NE) was defined by the aftershock sequence, which includes 858 aftershocks of magnitude greater than 2  $M_L$  that occurred the first seventeen days. The distribution of hypocentres in cross section does not immediately suggest a planar distribution but rather defines a volume about 15 km (depth) by 35 km (NW-SE) and by 20 km (NE-SW).

**Key words:** Major earthquakes, Gulf of Corinth, seismotectonics.

### 1. Introduction

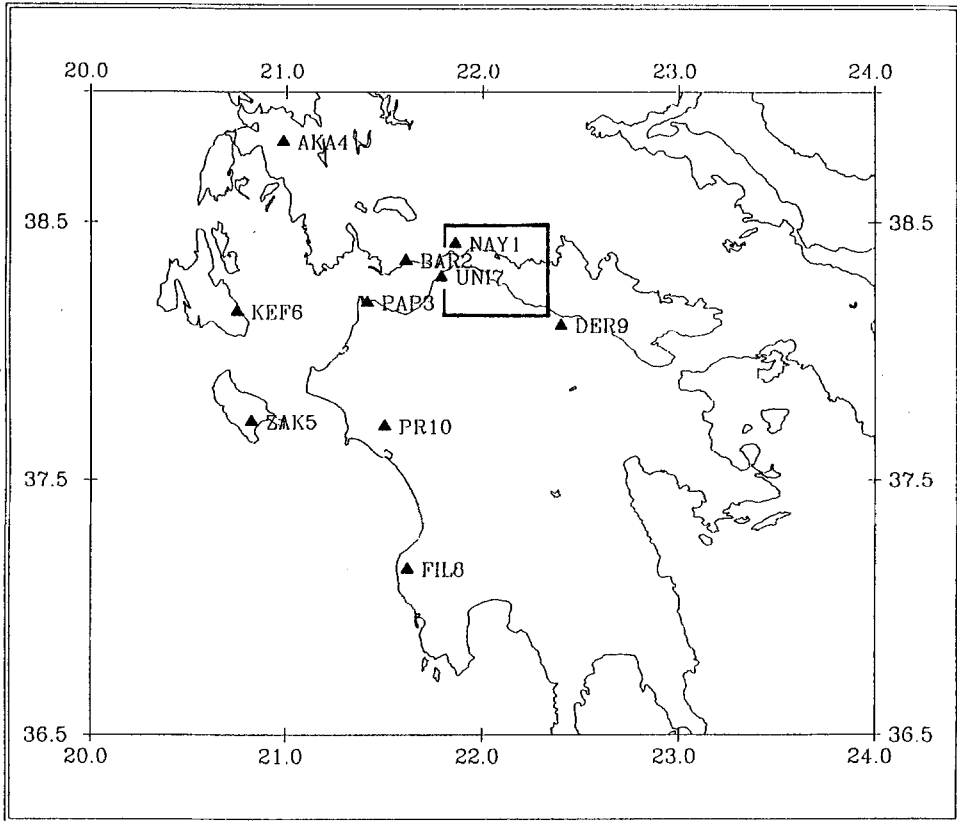
A large earthquake of magnitude 6.2  $M_L$  occurred on June 15, 1995 at 00:15 GMT in the western end of the Gulf of Corinth, and devastated the city of Egion, where one blockbuilding in the town centre, and one hotel at the eastern outskirts of the city in the village of Valimitica, collapsed, killing twenty-six people. This earthquake was followed 15 min later by a large aftershock of magnitude 5.4  $M_L$ .

More than 200 people were injured. Considerable damage occurred in the cities of Egion, Eratini and in many villages around the western end of the Gulf of Corinth, on both the southern and northern sides of the Gulf.

At the time of the events, the recently established permanent Seismological Network of the University of Patras (hereafter PATNET) was operating. This recorded continuously all the aftershock activity. In this note we present the earthquake sequence during the first seventeen days after the main event, as recorded by PATNET, and we attempt an interpretation in relation to the prevailing tectonics in the region.

---

<sup>1</sup> Seismology Laboratory, University of Patras, Rio 261 10, Greece.



The University of Patras Seismic Network (PATNET)

Figure 1

The station distribution of PATNET which recorded the Egion earthquake sequence. The box denotes the Egion area.

## 2. Instrumentation

The University of Patras Seismic Network (PATNET) covers the region of western Greece (Figure 1). It consists of nine stations, each with one vertical component short-period (1 Hz) seismometer operating at 60 dB dynamic range in a low noise environment. The signals are radiolinked using FM subcarriers to the central recording site at the University of Patras, where a three-component seismometer station is located. There, each channel is antialias filtered with a 30 Hz Butterworth low-pass filter, sampled at 100 Hz and converted to digital form with a resolution of 32 bits. A GPS is used as the timing base of the recording system.

Table 1  
*The P velocity model used for location*

Depth (km)	Velocity (km/sec)
0– 5	5.7
5–18	6.0
18–39	6.4
39–∞	7.9

### 3. Data Analysis

For the initial phase picking and data processing, SISWIN (TSELENTIS *et al.*, 1994b) was used while for the event location and magnitude calculation the HYPO71PC program (LEE and LAHR, 1975; LEE and VALDES, 1985) was used.

Initially, 858 aftershocks with magnitude greater than  $2 M_L$  were selected on the basis that these were recorded in at least 5 stations and had RMS travel time residual less than 0.25 s. A further discrimination was based on the signal-to-noise ratio, keeping only those seismograms which had a S/N ratio greater than 5. *P*- and *S*-wave arrival times were read with an accuracy better than 0.02 s and 0.07 s, respectively. This was achieved by employing the features of SISWIN that are particularly convenient for arrival picking, zooming and noise reduction.

The velocity model used for locating the aftershocks was that proposed by TSELENTIS *et al.* (1994a) and is used by PATNET on a routine basis (Table 1). The locations accepted were allowed a maximum error of less than 3 km on both epicentre and focal depth, and RMS travel time residuals less than 0.20 s. Averages of the standard hypocentral errors indicates  $\pm 2.1$  km for the horizontal and  $\pm 2.6$  km in depth (ERH and ERZ, respectively, in the HYPO71 standard error statistics). Although these expressed standard errors do not represent actual error limits (BOYD and SNOKE, 1984), use of *S*-phase data improves considerably the location accuracy. In total, 293 events were finally adopted as well-located and their hypocentral data are given in Table 2.

The magnitude reported for all the events is the local duration magnitude  $M_L$ , calculated from total signal duration following LEE *et al.* (1972), using the following equation (after KIRATZI and PAPAACHOS, 1985; TSELENTIS *et al.*, 1994a):

$$M_L = 2.32 \text{ Log}(T) + 0.0013D + C$$

where  $T$  is the signal duration in seconds,  $D$  is the epicentral distance in km and  $C$  a constant, different for each station.

Table 2  
*List of the 293 well-located events*

Date	Origin	Lat.°N	Long.°E	Depth	Mag.
950615	015 50.90	38–18.54	22– 8.46	12.78	6.21
950615	030 51.80	38–15.19	22– 5.92	1.17	5.37
950615	058 53.29	38–13.67	22– 8.88	1.25	3.28
950615	1 3 28.13	38–21.20	21–36.55	7.00	3.15
950615	136 43.44	38–11.91	22–17.34	3.29	3.28
950615	149 36.11	38–12.21	22–19.80	3.65	3.39
950615	151 31.71	38–16.71	22– 1.91	1.27	3.51
950615	157 17.21	38– 9.73	22–16.07	0.21	2.59
950615	2 8 52.61	38–14.43	22–17.96	0.48	2.75
950615	236 5.90	38–18.97	22– 7.39	0.42	3.24
950615	238 5.40	38–13.55	22–15.77	3.45	3.45
950615	241 38.53	38–13.37	22–11.46	11.88	3.16
950615	248 16.05	38–16.12	22–11.78	7.68	3.05
950615	334 1.23	39–18.17	22– 0.02	0.93	2.99
950615	443 13.73	38–16.89	22– 0.49	1.56	3.17
950615	451 21.17	38–13.81	22– 5.41	0.03	4.71
950615	5 1 38.37	38–48.52	22–17.49	3.53	3.24
950615	513 26.62	38–14.33	22– 6.42	0.15	2.82
950615	524 26.99	38–21.64	21–51.67	0.73	2.58
950615	535 21.58	38–25.10	21–51.67	7.00	2.77
950615	551 48.16	38–20.14	22– 3.25	0.30	2.98
950615	6 5 53.28	38–18.48	22– 5.51	0.05	2.88
950615	658 43.17	38–18.57	22– 6.24	0.64	3.00
950615	7 1 2.51	38–18.72	22– 0.09	7.00	4.03
950615	712 12.77	38–17.03	22– 3.33	1.67	3.14
950615	720 10.14	38–19.94	21–58.99	0.13	3.18
950615	724 2.98	38–15.22	22– 9.09	1.10	2.69
950615	741 35.21	38–18.93	22– 6.43	3.07	3.04
950615	758 7.85	38–10.88	22–31.02	2.38	2.85
950615	816 31.96	38–11.37	22–26.03	1.55	3.32
950615	822 36.32	38–19.96	21–59.94	0.21	2.98
950615	833 18.65	38–14.01	22–10.95	0.87	2.84
950615	958 1.80	38– 4.87	22– 0.57	13.21	2.97
950615	10 2 36.40	38–13.04	21–51.67	1.18	2.84
950615	10 3 49.45	38–17.42	21–59.27	0.66	3.25
950615	10 8 2.60	38–18.12	22– 2.66	0.73	2.90
950615	1012 18.51	38–25.10	21–40.77	7.00	2.34
950615	1033 36.80	38–17.24	22– 1.23	6.96	3.12
950615	1041 51.91	38–16.67	22– 1.05	0.22	4.13
950615	1058 12.83	38–34.91	22– 3.02	29.28	2.42
950615	11 5 45.45	38–35.94	21–54.52	11.40	2.28
950615	1228 44.93	38–32.87	21–58.37	0.69	3.07
950615	1255 26.17	38–24.45	22– 6.54	13.30	2.88
950615	1329 59.78	38–32.84	21–55.85	18.63	2.71
950615	1333 20.70	38–28.59	21–59.86	30.54	3.05
950615	1346 8.80	38–25.10	21–51.67	7.00	2.98
950615	1432 43.98	38–21.69	21–54.57	2.22	2.82
950615	1435 16.01	38–12.46	22– 7.72	1.46	3.26
950615	1451 1.18	38–17.05	22– 6.47	0.41	2.85

Table 2--Continued

Date	Origin	Lat. °N	Long. °E	Depth	Mag.
950615	15 6 35.48	38-42.95	21-58.23	0.10	4.25
950615	1556 41.53	38-16.83	22- 5.43	0.90	2.88
950615	1620 33.21	38-23.91	22- 5.67	24.43	2.85
950615	1631 19.29	38-34.27	21-54.90	13.27	2.77
950615	1657 26.70	38-14.73	22- 3.71	5.61	3.19
950615	1720 6.22	38-18.90	21-58.30	1.58	3.28
950615	1749 56.15	38-14.96	22-12.81	0.29	3.02
950615	1755 28.64	38-19.60	21-56.66	0.20	2.87
950615	1812 51.85	38-41.28	21-54.12	1.93	3.20
950615	1855 39.76	38-33.46	21-58.00	18.23	2.67
950615	1944 12.39	38-16.91	22- 1.90	0.32	3.46
950615	1959 41.25	38-23.74	21-51.67	7.00	3.31
950615	2136 42.92	38-38.66	21-57.96	21.10	3.25
950615	2152 44.33	38-22.86	21-51.05	5.57	2.84
950615	22 1 35.99	38-45.99	22-11.95	6.94	3.37
950615	2232 38.69	38-17.37	22- 4.91	0.85	2.95
950615	2237 59.07	38-23.54	21-52.35	7.00	3.08
950615	2326 27.88	38-20.47	22- 0.74	0.11	2.82
950616	021 33.36	38-41.15	22-12.44	13.96	3.05
950616	050 33.15	38- 9.46	21-55.77	18.98	3.10
950616	054 16.04	38-28.89	21-50.69	0.99	3.14
950616	058 55.35	38-32.20	21-55.08	14.35	2.65
950616	129 7.29	38-25.33	21-54.59	12.53	2.86
950616	231 13.73	38- 3.27	22- 8.49	25.76	2.76
950616	252 35.62	38-19.93	21-57.93	11.31	3.17
950616	3 3 14.36	38-22.64	21-50.83	1.81	3.33
950616	623 33.59	38-17.10	22-10.08	5.95	2.56
950616	720 39.37	38-14.25	22-11.31	4.92	3.23
950616	727 11.43	38-11.02	22- 8.60	6.39	3.53
950616	731 59.86	38-17.25	22- 8.80	0.40	2.60
950616	824 33.99	39-12.56	22-17.65	5.41	3.44
950616	834 46.03	38-25.10	21-51.67	7.00	2.28
950616	1028 53.61	38-25.10	21-51.67	7.00	2.03
950616	1045 59.14	38-14.17	22-11.79	9.59	3.35
950616	1250 24.89	38-19.49	21-57.38	1.89	3.34
950616	1554 34.53	38-21.34	21-53.66	2.15	3.18
950616	1637 53.19	38-12.18	22- 2.38	10.44	3.14
950616	1640 21.20	38-18.20	21-58.93	0.63	4.05
950616	1711 43.48	38-37.19	22- 0.35	12.40	2.64
950616	1719 15.57	38-14.96	22- 1.24	0.71	3.28
950616	1726 36.71	38-21.66	22- 6.78	15.03	3.19
950616	1816 1.18	38-16.61	22- 5.72	1.00	3.05
950616	1823 11.71	38-17.63	22- 6.09	0.30	3.61
950616	1838 6.57	38-21.25	21-59.28	0.13	3.00
950616	1846 31.41	38-10.82	22-12.90	0.27	3.70
950616	1850 50.39	38-19.23	21-59.31	0.81	3.30
950616	1853 54.70	38-40.78	21-52.91	19.26	3.10
950616	1929 48.25	38-18.61	21-59.44	0.78	3.64
950616	1937 11.49	38-29.03	21-52.68	8.91	2.88
950616	2032 5.58	38-21.39	22- 3.63	2.62	3.10

Table 2—Continued

Date	Origin	Lat. °N	Long. °E	Depth	Mag.
950616	2040 18.01	38–12.26	22–18.01	0.50	3.04
950616	2050 1.32	38–20.01	22– 1.03	0.78	2.76
950616	21 0 24.80	38–14.91	22– 1.61	0.32	3.19
950616	2237 59.92	38–16.79	22– 4.67	0.33	3.12
950616	2242 18.42	38–16.52	22– 6.94	0.38	2.76
950616	2256 3.53	39–19.22	22– 2.91	7.00	3.14
950616	23 2 50.78	38–11.12	22–12.65	1.23	3.42
950616	2323 49.12	38–30.24	21–51.51	7.00	2.99
950617	0 6 22.69	38–16.81	22– 2.71	0.57	3.05
950617	121 59.08	38–16.00	22– 4.86	0.05	3.15
950617	216 34.23	38–15.38	22–27.98	0.40	2.79
950617	443 26.08	38–25.10	21–54.04	13.85	2.68
950617	457 41.63	38–17.73	22– 8.34	8.93	2.91
950617	653 6.20	38–15.92	22– 9.22	2.56	3.23
950617	8 8 37.45	38–19.05	22– 5.79	5.08	3.07
950617	837 27.55	38–16.69	22– 9.16	8.18	3.06
950617	851 23.76	38–12.08	22–17.99	4.04	3.41
950617	944 15.71	38–15.20	22– 9.68	6.35	3.24
950617	1011 51.98	38–11.37	22– 4.39	0.88	3.21
950617	1018 4.15	38–21.09	22– 3.09	7.00	3.25
950617	1055 12.10	38–21.74	22–12.57	2.13	3.00
950617	11 3 19.43	38–18.90	22–11.04	12.38	3.58
950617	1112 0.89	38–15.83	22– 5.15	0.37	3.62
950617	1120 57.48	38–16.61	22–14.00	5.24	3.65
950617	1420 32.38	38–18.57	22– 2.25	0.49	3.66
950617	1321 23.37	38–30.54	21–51.56	10.49	2.32
950617	1346 26.47	38–17.15	22–10.95	3.12	3.28
950617	1410 30.24	38–15.92	22– 4.13	1.57	3.04
950617	1424 29.45	38–18.35	22– 0.41	0.05	3.32
950617	1437 34.63	38–16.02	22– 3.92	5.18	3.01
950617	1454 24.32	38–16.80	22– 2.95	0.54	3.31
950617	1526 21.95	38–25.10	21–51.67	7.00	2.45
950617	1555 54.54	38–18.95	22– 2.71	0.29	3.13
950617	16 7 41.76	38–17.29	22– 9.52	3.33	3.30
950617	1637 29.95	38–19.54	21–59.17	5.76	2.94
950617	1947 25.08	38–21.99	21–53.59	0.27	3.32
950617	2039 0.37	38– 1.69	22– 7.11	0.36	3.30
950617	2053 41.32	38–22.97	21–37.50	30.39	2.71
950617	2230 59.12	38–17.63	22– 6.21	11.96	3.91
950617	2310 23.45	38–16.41	21–58.66	1.45	3.26
950617	2337 14.69	39–17.45	21–57.79	0.80	3.30
950618	034 40.98	38–17.83	21–59.38	1.11	3.02
950618	038 8.72	38–16.24	22–12.62	1.05	3.30
950616	114 7.57	38–16.95	22– 2.63	0.90	4.22
950618	117 38.02	38–17.64	22– 6.11	0.05	2.86
950618	148 4.93	38–21.28	22– 6.01	0.40	2.76
950618	241 57.97	38–18.57	22–12.38	4.65	3.02
950618	324 55.48	38–14.82	22–14.96	2.69	3.48
950618	354 0.05	38–17.37	22– 4.61	1.55	3.69
950618	357 19.66	38–16.46	22–10.35	2.81	2.99

Table 2—Continued

Date	Origin	Lat. °N	Long. °E	Depth	Mag.
950618	4 0 48.75	38–18.43	22– 6.03	2.87	3.52
950618	428 25.84	38–18.48	21–59.49	0.48	4.42
950618	440 16.77	38–33.06	21–51.67	7.00	3.06
950618	447 21.58	38–19.03	21–57.86	0.60	3.57
950618	452 7.27	38–16.84	22– 3.77	11.29	3.86
950618	6 4 50.58	38–21.70	21–51.87	1.81	3.15
950618	6 7 51.45	38–22.24	22– 0.82	0.73	3.22
950618	615 37.25	38–34.49	21–59.70	19.00	2.60
950618	616 18.19	38–32.81	21–58.03	17.99	2.63
950618	639 3.68	38–16.27	22– 1.01	0.68	2.93
950618	657 2.50	38–34.19	21–54.73	7.15	2.62
950618	8 6 1.47	38–25.10	21–52.03	8.69	2.86
950618	834 51.06	38–29.53	21–57.93	14.23	3.66
950618	1053 59.22	38–17.15	21–57.74	0.67	3.50
950618	12 8 49.76	38–11.26	22–18.35	8.83	3.71
950618	1222 4.16	38–25.10	21–51.67	7.00	2.73
950618	1247 22.26	38–22.82	21–56.48	0.57	3.15
950618	1352 36.70	38–17.85	21–59.07	0.55	3.72
950618	1441 7.34	38–42.87	22– 3.20	6.32	2.21
950618	1445 34.02	38–25.10	21–51.67	7.00	3.34
950618	1413 8.19	38–16.10	22– 8.92	0.41	3.03
950618	1751 22.85	38–25.10	21–51.67	7.00	3.29
950618	1858 56.18	38–12.56	22–15.77	0.94	3.12
950618	19 3 13.00	38–20.83	21–58.37	0.25	2.99
950618	2015 9.96	38–19.16	21–56.26	1.07	3.53
950618	22 8 38.84	38–16.32	22– 1.58	1.74	3.27
950619	021 15.02	38–18.29	22– 5.62	0.18	3.15
950619	420 21.76	38–24.44	21–52.73	0.51	2.90
950619	619 18.20	38–13.14	22– 8.89	5.34	3.93
950619	745 3.29	38–29.32	21–56.93	17.39	2.54
950619	834 45.67	38–27.95	21–50.62	8.61	2.42
950619	1029 24.17	38–28.45	21–54.80	14.12	2.78
950619	1034 8.84	38–31.85	22– 0.27	3.00	2.79
950619	1048 49.52	38–25.10	21–51.67	7.00	2.82
950619	1421 6.44	38–17.87	22–21.74	6.42	3.43
950619	1635 21.33	38–25.40	21–49.55	3.70	2.68
950619	1723 31.05	38–13.40	22– 9.36	4.58	3.17
950619	20 8 30.67	38–19.92	22– 0.77	2.57	3.34
950619	2054 25.94	38–13.44	22–18.91	4.61	3.27
950619	2220 37.22	38–18.94	22– 7.79	11.71	2.79
950619	2322 18.17	38–13.40	22–12.21	4.68	3.01
950620	151 26.04	38–31.89	21–30.02	24.01	2.36
950620	326 49.49	38–13.02	22– 0.97	1.15	3.04
950620	358 22.43	38–16.25	21–58.33	0.46	3.25
950620	616 6.50	38–16.97	22– 0.87	0.46	3.15
950620	623 36.57	38–20.05	22–10.41	0.83	3.18
950620	631 37.30	38–17.45	21–56.63	0.26	3.47
950620	636 48.05	38–27.87	21–37.22	14.05	3.63
950620	13 0 18.64	38–13.76	22– 8.50	0.26	3.51
950620	820 35.78	38–17.24	22–10.29	12.50	2.82

Table 2—Continued

Date	Origin	Lat.°N	Long.°E	Depth	Mag.
950620	1047 1.85	38–13.44	22– 1.77	0.68	3.00
950620	1215 47.85	38– 5.70	22– 8.26	13.24	3.22
950620	1217 47.97	38– 1.12	22–11.00	9.34	3.35
950620	1349 55.10	38–15.92	22– 6.58	2.63	2.80
950620	1438 31.01	38–15.38	22–17.89	5.43	3.66
950620	16 7 26.64	38–16.68	22–15.47	0.06	3.66
950620	2021 42.18	38–17.15	22– 9.55	12.64	3.52
950620	2232 3.79	38–21.45	22–14.48	2.76	2.85
950621	0 2 0.87	38–17.69	22– 6.71	9.82	3.07
950621	1 3 17.10	38–14.56	22–21.34	3.23	3.60
950621	224 23.21	38–12.49	22–21.82	0.14	3.66
950621	523 13.90	38–16.13	22– 2.62	0.19	3.08
950621	530 23.63	38–17.09	22– 5.94	1.04	3.63
950621	6 6 27.55	38–24.02	21–51.93	7.00	2.70
950621	949 39.25	38–24.30	21–52.89	8.21	2.74
950621	1248 1.09	38–20.42	21–53.21	0.57	2.52
950621	1332 9.84	38–18.71	22–11.45	7.05	3.24
950621	15 1 8.14	38–19.17	22– 1.51	1.43	3.62
950622	250 2.83	38–25.10	21–51.67	7.00	2.93
950622	442 44.84	38–19.67	21–54.46	3.71	3.35
950622	445 0.45	38–17.68	21–57.15	0.91	3.14
950622	658 30.87	38–17.64	21–59.86	0.63	3.36
950622	7 8 27.69	38–17.50	22– 0.94	0.05	3.81
950622	942 4.03	38–22.15	21–51.67	3.82	3.10
950622	950 33.49	38–28.54	21–55.00	12.93	2.86
950622	11 8 56.14	38–25.10	21–51.77	7.22	2.65
950622	1428 53.08	38–18.55	22– 1.44	0.51	3.55
950622	17 9 41.87	38–18.90	22– 2.14	7.00	2.83
950622	1714 55.21	38–16.69	22– 4.54	5.10	2.76
950622	1742 31.07	38–18.94	21–56.86	0.55	2.78
950622	2311 1.77	38–32.30	21– 4.30	7.29	2.65
950623	314 29.90	38–18.15	21– 1.43	26.78	2.52
950623	824 7.16	38–25.83	21– 2.30	7.27	3.09
950623	855 20.71	38–25.10	21– 1.67	7.00	2.75
950623	10 8 1.33	38–29.76	21– 9.77	2.25	2.54
950623	1432 54.07	38–12.24	22– 7.55	0.14	3.59
950623	2130 5.59	38–16.79	22– 8.73	0.40	3.28
950623	3241 15.27	38–25.10	21–58.98	11.73	3.01
950624	744 26.18	38–20.08	21–40.53	4.41	2.74
950624	1316 56.83	38–15.96	21–58.69	2.56	3.97
950624	1327 22.07	38–21.02	22– 8.52	13.34	3.83
950624	1934 13.90	38–15.13	22–12.37	3.35	3.13
950624	22 4 55.75	38–25.10	21–51.67	7.00	3.24
950625	2 1 26.62	38–19.08	22–10.02	11.96	3.08
950625	213 59.08	38–16.16	22– 4.21	0.16	3.14
950625	242 37.33	38–17.10	22–15.61	8.61	3.59
950625	7 5 55.15	38–25.10	21–52.58	9.41	2.62
950625	955 43.28	38–29.97	21–58.18	18.91	2.52
950625	1412 54.83	38–13.92	22– 4.81	0.29	3.56
950625	1415 58.22	38– 9.39	22– 9.87	0.36	3.27



Table 2—Continued

Date	Origin	Lat. °N	Long. °E	Depth	Mag.
950625	15 4 17.32	38–15.76	21–57.86	0.84	3.21
950625	1532 42.82	38–18.54	21–58.55	0.78	2.85
950625	1542 24.35	38–14.88	22– 4.75	3.02	3.07
950625	16 6 52.95	38–27.78	21–50.27	7.00	2.65
950625	1616 36.08	38–28.26	21–51.96	7.00	2.72
950625	1718 4.56	38–13.01	22– 6.74	7.99	3.26
950625	1817 7.96	38–17.12	21–58.72	0.19	2.76
950625	2038 11.21	38–12.92	22– 2.70	0.23	3.25
950626	149 16.22	38–13.28	22– 6.98	2.67	3.40
950626	152 58.43	38–13.03	22– 4.44	0.48	3.54
950626	324 48.62	38–15.72	22– 5.69	0.27	2.89
950626	537 46.09	38–22.74	21–51.67	0.70	2.72
950626	643 41.48	38–25.10	21–53.81	12.18	2.72
950626	7 4 24.21	38–22.26	21–51.67	4.37	2.93
950626	853 49.60	38–23.57	21–53.21	9.19	2.54
950626	11 0 41.85	38–18.55	21–54.71	2.00	3.31
950626	1251 34.40	38–25.10	21–51.67	7.00	2.44
950626	1850 4.72	38–16.26	22–15.28	2.07	3.39
950626	2049 53.69	38–17.49	21–59.88	0.53	2.99
950626	2244 40.39	38–16.21	22– 1.54	1.02	2.84
950627	1420 44.30	38–20.23	21–54.21	3.24	3.23
950628	318 24.73	38–19.03	21–57.03	0.47	3.26
950628	424 58.28	38–17.80	22– 2.92	0.24	3.11
950628	547 32.25	38–17.88	21–57.75	1.36	2.66
950628	18 8 12.01	38–24.39	21–51.30	2.89	3.14
950628	1839 30.02	38–15.13	22– 4.68	11.97	3.29
950629	1036 34.51	38–21.05	21–56.15	0.34	2.77
950629	1053 14.34	38–25.10	21–53.34	11.34	2.88
950629	15 4 23.07	38–14.70	21–59.69	1.09	2.89
950629	1756 8.47	38–19.89	21–56.91	0.82	2.82
950629	2326 52.67	38–16.75	22– 2.23	0.10	3.06
950630	2 5 22.20	38–14.56	22– 2.11	1.24	2.55
950630	333 32.06	38–24.29	21–50.26	0.40	3.03
950630	342 23.02	38–15.60	22– 5.56	1.42	2.91
950630	5 1 47.95	38–19.87	21–55.48	0.15	3.09
950630	515 24.53	38–19.88	21–58.63	1.22	3.31
950630	2036 0.23	38–28.22	21–50.28	1.79	2.58
950701	253 32.32	38–25.10	21–51.67	7.00	2.51
950701	517 4.53	38–20.96	21–54.25	1.02	2.63
950701	1413 10.52	38–16.97	22– 3.05	7.00	2.81
950701	19 8 34.06	38–18.37	21–58.53	0.45	3.27
950701	2022 41.98	38–12.11	22–15.39	4.27	3.99
950701	2158 6.45	38–15.98	22– 1.61	0.13	4.35
950701	2247 36.51	38–17.56	22– 6.91	5.46	3.30

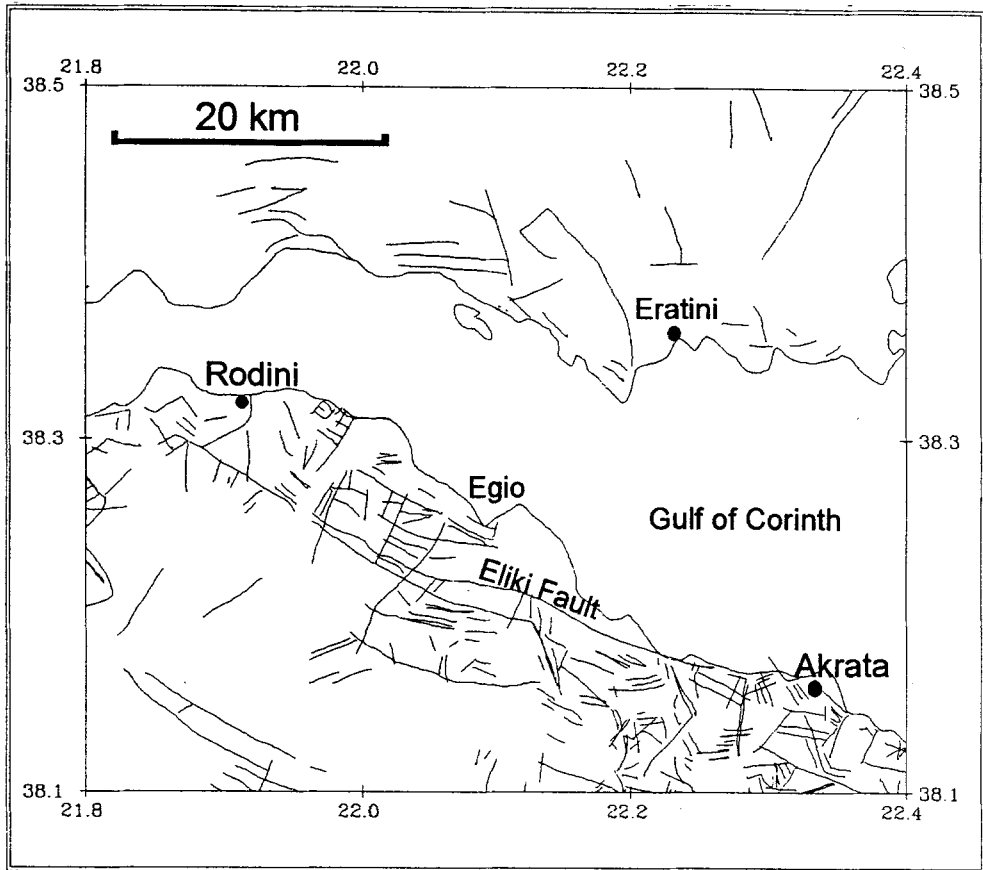


Figure 2

Neotectonic faulting in the Egion area (after DOUTSOS and PIPER, 1990; COLLIER and DART, 1991; ROBERTS and JACKSON, 1991; DOUTSOS and POULIMENOS, 1992; POULIMENOS, 1993).

#### 4. Regional Setting

The Gulf of Corinth occupies a zone of crustal extension, which is an integral part of the Aegean Orogene, and has long been recognised as an asymmetric graben structure formed by normal faulting and a region of pronounced seismicity (BROOKS and FERENTINOS, 1994).

Several studies have been conducted on this graben system. BROOKS and FERENTINOS (1984) and HIGGS (1988) studied the structure of the Corinth graben offshore. They showed the WNW-ESE master fault that defines the graben to the South and the faults forming the hangingwall. Onshore studies (e.g., JACKSON *et al.*, 1982; VITA-FINZI and KING, 1985; KING *et al.*, 1985; DOUTSOS and PIPER, 1990; COLLIER and DART, 1991; ROBERTS and JACKSON 1991; DOUTSOS and

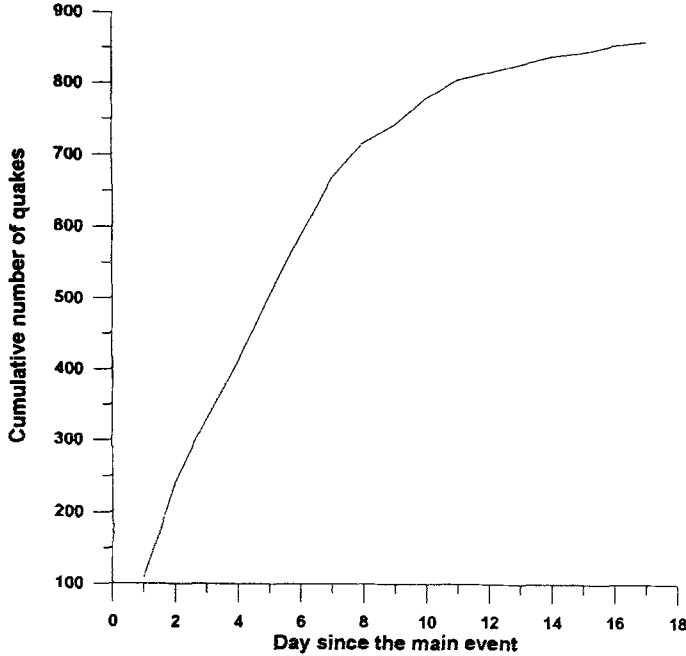
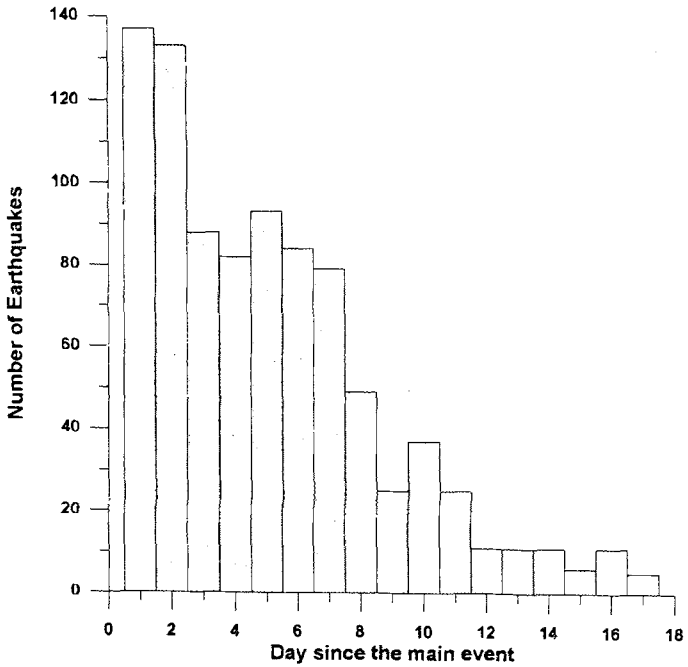
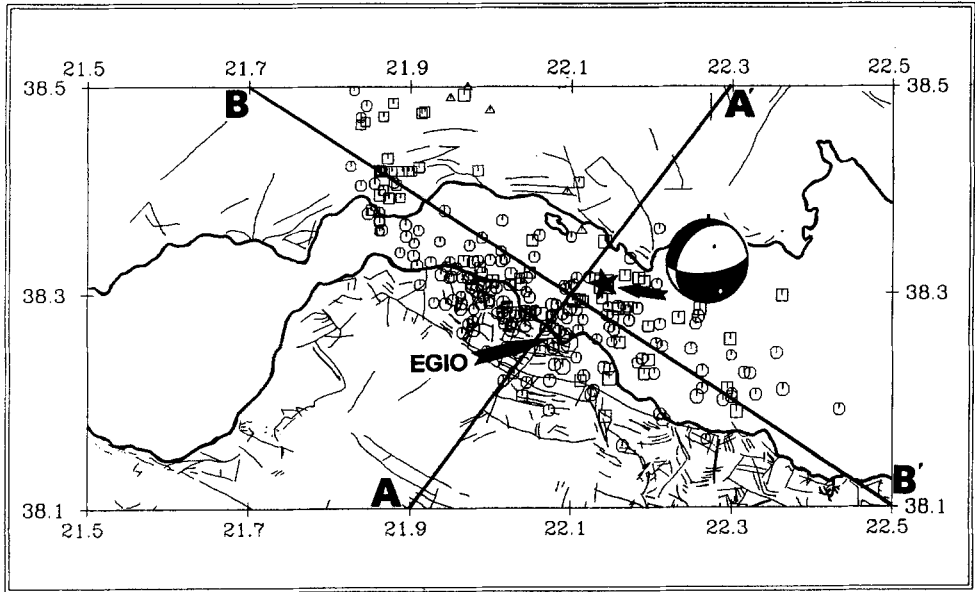
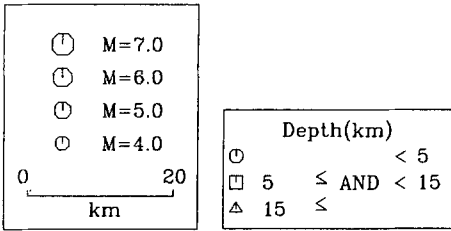


Figure 3

Time evolution of the aftershock sequence for seventeen days after the main event. 858 events are considered with magnitude  $M_L > 2$ . (a) Time distribution of the number of events per day, (b) cumulative time distribution of events.



15/06/95 - 01/07/95

Figure 4

Spatial distribution of the 293 well-located events during the first seventeen days of the aftershock sequence. The star denotes the main shock and the focal mechanism solution presented is after NEIC (USGS, 1995). AA' and BB' the cross sections presented in Figure 5.

POULIMENOS, 1992; POULIMENOS, 1993; ABERCROMBIE *et al.*, 1985) showed that the tectonic regime to the south and east of the Gulf is dominated by normal faulting of WNW-ESE trend, where as at the western end E-W trending normal faults are dominant. Figure 2 presents the neotectonic faulting at the area of Egion.

MELIS *et al.* (1989) proposed a model resulting from microseismicity studies. This shows the probable extension of the Gulf of Corinth WNW towards Trichonis Lake, and the Gulf of Patras as a graben of similar trend but offset by the transtensional structure of the NE-SW trending Rio graben to the west of the Corinth Gulf (BROOKS *et al.*, 1988).

A deepening zone of microearthquake hypocentres towards the NE mapped the master fault and the hangingwall activity at the western end of the Gulf of Corinth

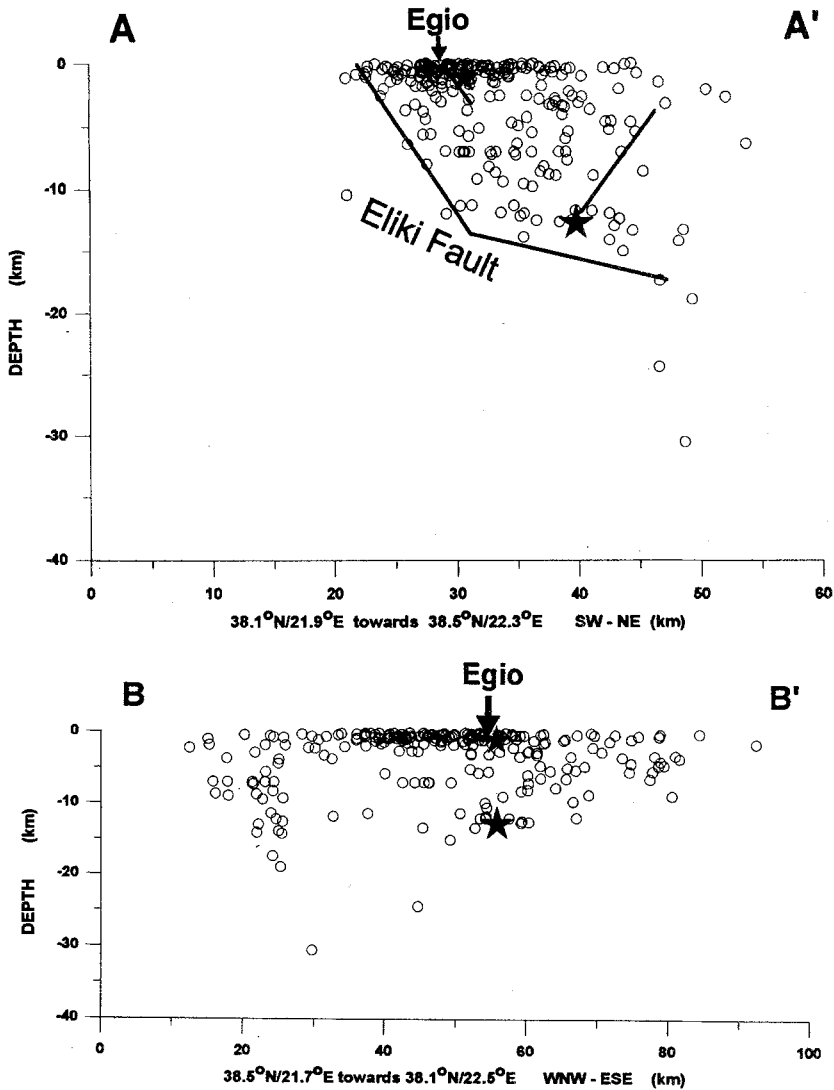


Figure 5

(a) *AA'* SW-NE cross section, (b) *BB'* WNW-ESE cross section. Both shown in Figure 4. The big star denotes the main event and the small the largest aftershock. Both faults corresponding to the fault plane solutions referred to in the text are shown in (a).

(MELIS *et al.*, 1989; HATZFELD *et al.*, 1990). Since then, several microseismicity studies have confirmed these findings and similarly the present publication does also. However, it is also important to note that MELIS *et al.* (1995) have reported “anomalous” events in this area. These anomalous events have relatively higher seismic moments and lower stress drop and coseismic slip values in relation to the rest of the events located in the same region. They also calculated higher values of fault radius, suggesting that longer faults produce this type of event.

	PHI	DIP	RAKE	TREND	PLUNGE
A:	72.0	79.0	-53.6	T: 134.4	25.1
B:	176.5	37.8	-161.9	P: 17.6	43.9

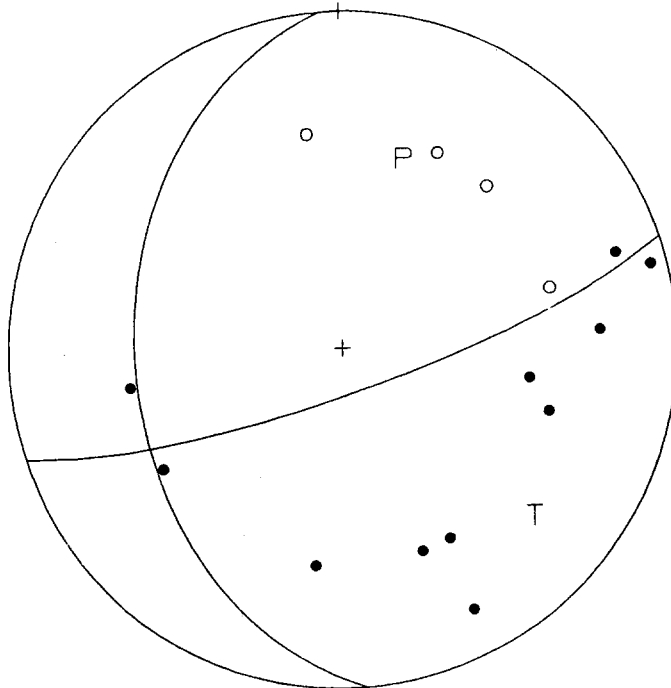


Figure 6

Fault plane solution of the main event derived from *P* onsets recorded at PATNET and the National Greek Network.

### 5. The Aftershock Sequence

The time evolution of the aftershock sequence for seventeen days after the main event is shown in Figures 3a and b, where all the events with magnitude  $M_L > 2$  are considered. Thus, the time distribution of the cumulative number of aftershocks (Figure 3a) and the total number of earthquakes per day (Figure 3b) are presented.

The principal spatial characteristics of the 293 located aftershocks are illustrated in Figures 4 and 5a,b. This distribution of hypocentres in cross section does not immediately suggest a planar distribution but rather defines a volume about 15 km (depth) by 35 km (NW-SE) and by 20 km (NE-SW).

As shown on the *AA'* cross section (Figure 5a), the main shock and the larger aftershock occurred on different faults, the second activated by the first. The

fault plane solution suggested by NEIC (USGS, 1995) and shown in Figure 4 is similar to the one estimated using PATNET first onsets in conjunction with those reported by the National Observatory of Athens (1995) and shown in Figure 6. This suggests a normal fault dipping towards the SSE with a dip angle of approximately 70 degrees as the main plane, which indicates a fault bounding the hangingwall to the north. Lack of first onsets for the second event limits further interpretation, but the focal depth and epicentre in conjunction with secondary effects at the surface and close to the city of Egion in particular (i.e., liquefaction, off-shore landslides, surface ruptures) suggest that it is also related to hangingwall faulting but dipping towards the NNE.

### 6. Conclusions

The Egion earthquake sequence, as it was recorded by PATNET, indicates a main event that occurred on a fault at the north side of the western end of the Gulf of Corinth, which bounds the hangingwall to the north, and it was followed by the largest aftershock that occurred near the city of Egion, possibly on a fault parallel to the Eliki fault at a shallower depth.

### Acknowledgements

We are grateful to Dr. P. W. Burton (collaborating under NATO CRG 940718) and Dr. D. Seber who critically reviewed this manuscript.

### REFERENCES

- ABERCROMBIE, R. E., MAIN, I. G., DOUGLAS, A., and BURTON, P. W. (1995), *The Nucleation and Rupture Process of the 1981 Gulf of Corinth Earthquakes from Deconvolved Broad-band Data*, *Geophys. J. Int.* 120, 393–405.
- BOYD, T. M., and SNOKE, A. J. (1984), *Error Estimates in Some Commonly Used Earthquake Location Programs*, *Earthquake Notes* 55 (2), 3–6.
- BROOKS, M., CLEWS, J. E., MELIS, N. S., and UNDERHILL, J. R. (1988), *Structural Development of Neogene Basins in Western Greece*, *Basin Res.* 1, 129–138.
- BROOKS, M., and FERENTINOS, G. (1984), *Tectonics and Sedimentation in the Gulf of Corinth and the Zakynthos and Kefallinia Channels, Western Greece*, *Tectonophysics* 101, 25–54.
- COLLIER, R. E. LL., and DART, C. J. (1991), *Neogene to Quaternary Rifting, Sedimentation and Uplift in the Corinth Basin, Greece*, *J. Geol. Soc.* 148, 1049–1065.
- DOUSOS, T., and PIPER, D. J. W. (1990), *Listric Faulting, Sedimentation and Morphological Evolution of the Quaternary Eastern Corinth Graben: First Stages in Continental Rifting*, *Geol. Soc. of Am. Bull.* 102, 812–829.
- DOUSOS, T., and POULIMENOS, G. (1992), *Geometry and Kinematics of Active Faults and their Seismotectonic Significance in the Western Corinth-Patras Rift (Greece)*, *J. Struct. Geol.* 14, 689–699.
- HATZFELD, D., PEDOTTI, G., HATZIDIMITRIOU, P., and MAKROPOULOS, K. (1990), *The Strain Pattern in the Western Hellenic Arc Deduced from a Microearthquake Survey*, *Geophys. J. Int.* 101, 181–202.

- HIGGS, B. (1988), *Synsedimentary Structural Controls on Basin Deformation in the Gulf of Corinth, Greece*, *Basin Res.* 1, 155–165.
- JACKSON, J. A., GAGNEPAIN, J., HOUSEMAN, G., KING, G., PAPADIMITRIOU, P., SOUFLERIS, C., and VIRIEUX, J. (1982), *Seismicity, Normal Faulting and the Geomorphological Development of the Gulf of Corinth (Greece): The Corinth Earthquakes of February and March 1981*, *Earth and Planet. Sci. Lett.* 57, 377–397.
- KING, G. C. P., ONYANG, Z. X., PAPADIMITRIOU, P., DESCHAMPS, A., GAGNEPAIN, J., HOUSEMAN, G., JACKSON, J. A., SOUFLERIS, C., and VIRIEUX, J. (1985), *The Evolution of the Gulf of Corinth (Greece): An Aftershock Study of the 1981 Earthquakes*, *Geophys. J. R. Astr. Soc.* 80, 677–693.
- KIRATZI, A. A., and PAPAACHOS, B. C. (1985), *Local Richter Magnitude and Total Signal Duration in Greece*, *Annal. Geophys.* 3, 531–538.
- LEE, W. H. K., BENNETT, R. E., and MEAGHER, K. L. (1972), *A Method of Estimating Magnitude of Local Earthquakes from Signal Duration*, USGS, Open File Report, 1–28.
- LEE, W. H. K., and LAHR, J. C. (1975), *HYPO71 (Revised): A Computer Program for Determining Hypocentre, Magnitude, and First Motion Pattern of Local Earthquakes*, USGS, Open File Report, 85–749.
- LEE, W. H. K., and VALDES, C. M. (1985), *HYPO71PC: A Personal Computer Version of the HYPO71 Earthquake Location Program*, USGS, Open File Report, 1–28.
- MELIS, N. S., BROOKS, M., and PEARCE, R. G. (1989), *A Microearthquake Study in the Gulf of Patras Region, Western Greece, and its Seismotectonic Interpretation*, *Geophys. J. R. Astr. Soc.* 98, 515–524.
- MELIS, N. S., BURTON, P. W., and BROOKS, M. (1995), *Coseismic Crustal Deformation from Microseismicity in the Patras Area*, *Geophys. J. Int.* 122, 815–836.
- POULIMENOS, G. (1993), *Tectonics and Sedimentation in the Western Corinth Graben, Greece*, *N. Jb. Geol. Palaont. Mh.* 10, 607–630.
- ROBERTS, S., and JACKSON, J., *Active normal faulting in central Greece: An Overview*. In *The Geometry of Normal Faults* (eds. Roberts, A. M., Yielding, G., and Freeman, B.) (Geol. Soc. London Spec. Public. 56, 1991) pp. 125–142.
- TSELENTIS, G.-A., MELIS, N. S., and SOKOS, E. (1994a), *The Patras (July 14, 1993;  $M_s = 5.4$ ) Earthquake Sequence*, Presented at the 7th Congress of the Geol. Soc. of Greece, Thessaloniki, May 25–27.
- TSELENTIS, G.-A., XANALATOS, N., and MELIS, N. S. (1994b), *SISMWIN: A Computer Program for Seismological Data: Phase Picking and Processing*, Report C2, Patras Seismological Centre, 76 pp.
- VITA-FINZI, C., and KING, G. C. P. (1985), *The Seismicity, Geomorphology and Structural Evolution of the Corinth Area of Greece*, *Philos. Trans. of the Roy. Soc., London A314*, 379–407.

(Received July 14, 1995, accepted September 11, 1995)